I&EC research
Industrial & Engineering Chemistry Research
pubs.acs.org/IECR
Article

Comparison of Water- and Amine-Based Carbon Capture Processes for Air and Oxyfuel Combustion Technologies

Saeed Talei,* Agnes Szanyi, and Peter Mizsey

Cite This: *Ind. Eng. Chem. Res.* 2024, 63, 16486−16496

ABSTRACT: Carbon capture, utilization, and storage (CCUS) technologies can efficiently contribute to the mitigation of greenhouse gas emissions. Carbon capture with pressurized water is applied in the ammonia plant, and it has recently gained significant attention due to its environmentally friendly features. In this study, the technoeconomic evaluation of the water-based carbon capture system is carried out and compared with the alternative using aqueous MEA solution. The flue gas originates from a gas-fired power plant. Two options are considered: (i) an air-combustion system and (ii) an oxyfuel combustion system. The calculated results show that in both air and oxyfuel-combustion technologies, the power consumption of the H_2O-CO_2 capture method exceeds that of the MEA−CO_2 capture method by approximately 30% and 45%, respectively. This considerable difference notably increases the operational costs of the power plant. However, by the application of gas dehydration before the H_2O-CO_2 capture technique, the power consumption and the cost of water-based carbon capture can be significantly decreased. Although such an improvement makes the water-based carbon capture system the least energy consuming alternative, it requires mainly electricity and still has higher utility costs compared to MEA-based alternatives.

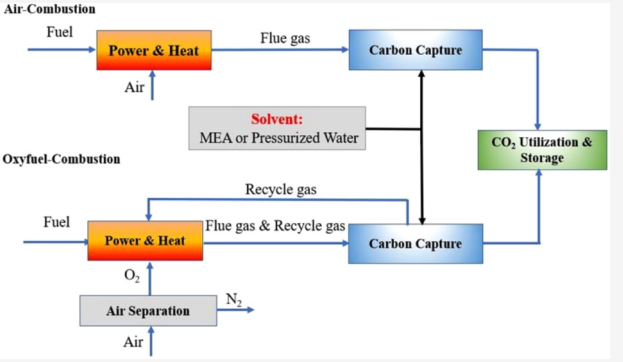

INTRODUCTION

The international interest in mitigating carbon dioxide emissions to combat climate change has been focusing attention on carbon capture, utilization, and storage (CCUS) technologies. CCUS is perceived as a crucial strategy to alleviate climate change.[1,2] CCUS is essential for achieving global climate goals and ensuring a sustainable future for generations to come. It offers an opportunity to address climate change while maintaining economic growth and energy security.[3,4] Carbon capture can play a critical role in permitting the continued use of fossil fuels, while limiting their environmental effect as we progress toward a more sustainable future. It enables us to decarbonize sectors that would otherwise be difficult to electrify or replace with renewable energy sources.[5,6] While renewable energy sources are rapidly growing, they still face challenges such as intermittency and storage limitations.[7,8]

While there have been successful pilot projects and some large-scale CCUS facilities in operation, the deployment of CCUS on a global scale is limited. One of the main challenges is the high cost associated with implementing CCUS technologies.[9,10] Additionally, there are concerns about the long-term storage of captured CO_2 and its potential leakage. However, many countries and organizations are investing in research and development to improve CCUS technologies and reduce costs.[11] There are three basic strategies for decreasing greenhouse gas emissions:[12,13] air-combustion, which occurs in the presence of air; oxyfuel burning, which occurs with fossil fuel rather than air; and precombustion, which occurs before combustion. These strategies can leverage a variety of CO_2 separation procedures. Absorption,[14,15] adsorption,[16] cryogenic separation,[17] and membrane[18] are examples of these. The most-often used technologies are absorption processes. CO_2 absorption can occur chemically or physically. In a chemical absorption process, aqueous alkanol amines are the most-often used chemical absorbents for CO_2 separation.[19] However, there are certain disadvantages to using aqueous alkanol amine absorbents, such as the high energy consumption for amine regeneration, the high rate of equipment corrosion, and the huge absorber capacity required.[20,21]

These research activities of carbon capture on gas-fired power plants were evaluated or studied at the pilot scale through process modeling designs.[22,23] Idem et al.[24] examined the performance of two different sources and compositions of

Received: June 13, 2024
Revised: July 25, 2024
Accepted: September 5, 2024
Published: September 13, 2024

https://doi.org/10.1021/acs.iecr.4c02216
Ind. Eng. Chem. Res. 2024, 63, 16486−16496

flue gas on a pilot scale utilizing aqueous MEA and mixed MEA/MDEA solvents. Their findings indicate that in the industrial setting of a CO_2 capture plant, using a mixed MEA/MDEA solution rather than a single MEA solution can result in a considerable reduction in energy demand.

The performance of an amine-carbonate mix with 30% MEA solvent from coal-derived flue gas in a pilot plant under identical experimental settings is tested and compared by Frimpong et al.[25] Under this circumstance, the combination appears to have the potential to reduce the energy penalty associated with utilizing industry standard MEA, as a solvent for CO_2 collection.

Several solvent families are being investigated, including amine-based,[26,27] carbonate-based,[28] aqueous ammonia (NH_3),[29,30] amino acid salts,[31] ionic liquids,[32] and deep eutectic solvents.[33] The conventional chemical absorption CO_2 capture technology is based on a main amine solvent, 30 wt % aqueous MEA, which has a low cost, high absorption capacity, and low regeneration heat requirement compared to others.[34] However, the degradation of amines with temperature and time, corrosion, amine losses by evaporation, and toxicity of solvents used in absorption processes are the drawbacks of this solvent.[35]

Furthermore, utilizing water to absorb CO_2 is a viable option; ammonia plants traditionally use pressurized water for carbon dioxide capture. On the other hand, seawater absorption is a natural technique of CO_2 capture. The seas are sucking the world's CO_2 out of the atmosphere at a pace of 300 tons per second.[36] According to Henry's law, all gases in the atmosphere, including CO_2, are soluble in water, and the solubility of gases in water is related to the partial pressure of the gas. CO_2 solubility in pure water is maximized at high pressures, and pressure swing desorption has occurred at low pressures. Recently, researchers examined the potential of pressurized water for CO_2 capture in industrial sections. Bayramŏlu[37] evaluated the performance of a process that used water as a physical solvent for the capture of CO_2 from flue gas in an off-shore postcombustion technology to improve CO_2 capture efficiency while reducing the energy requirement of the whole process. This aqueous CO_2 capture technique is extremely promising in terms of energy recovery and total cost reduction potential, and it produces CO_2 at a lower cost with no harmful degrading byproducts.[38]

While testing CO_2 capture systems on a large scale, process simulation programs such as Aspen Plus have been widely used to evaluate the process configurations and identify the optimum operating conditions.[39,40] Several studies used Aspen Plus to model the capture of CO_2 from different flue gas absorption processes. However, to the best of our knowledge, no such comparison between MEA solution and pressurized water in the absorption process has been conducted. Such a study is believed to be important, as water-based carbon capture has gained significant attention due to its potential to provide a baseline for efficient and cost-effective CO_2 removal.

In this work, using a rate-based model in Aspen Plus, a comprehensive analysis is carried out about the performance of novel water-based carbon capture. The power consumption and its costs, and solvent demands of these categories with conventional MEA−CO_2 capture processes in air and oxyfuel combustion technologies are modeled and compared. In total, there is a comparison of three different configurations as follows:

- MEA−CO_2 capture, which used a chemical MEA solution in a chemical absorption process.
- H_2O−CO_2 capture (strategy 1), in which CO_2 is captured using water as a physical solvent.
- H_2O−CO_2 capture + gas dehydration (strategy 2), in which flue gas dehydration occurred first, followed by CO_2 capture using water as a physical solvent.

METHODOLOGY AND SYSTEM MODELING

The study investigates and compares the absorption of 90% carbon dioxide from the flue gas of a gas-fired boiler using MEA and H_2O as solvents for chemical and physical absorption, respectively. The process block diagrams of these two technologies are presented in Figure 1. In the case of

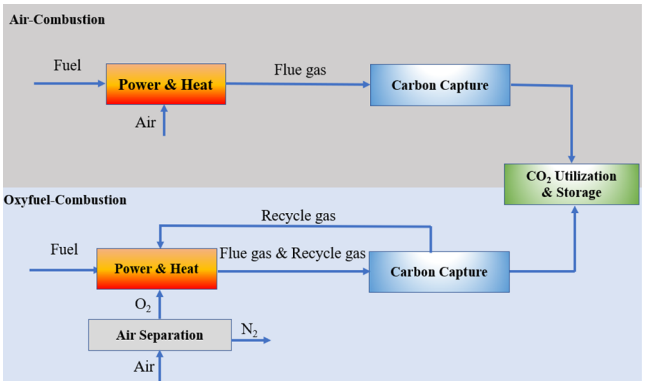

Figure 1. Schematic of the CO_2 capture process in air-combustion and oxyfuel-combustion technologies.

oxyfuel technology, where clean O_2 is used instead of air, the inert effect of nitrogen is replaced with additional carbon dioxide originating from the flue gas. In conventional oxyfuel technology, after the burning of fossil fuel in the presence of oxygen, a considerable amount of flue gas is recycled into the combustion chamber to regulate the temperature of the combustion process. In the proposed configuration, the flue gas recycling process occurs after the carbon capture absorber. In this situation, the absorption process's driving power of mass transfer is greater than that of the air-combustion process. In terms of chemical feasibility studies, the use of oxyfuel technology can provide the following benefits:

- Reduced energy requirements of regeneration due to greater CO_2 concentrations in the flue gas
- Lower demand for MEA solvents thanks to higher CO_2 concentrations
- Substituting nitrogen with carbon dioxide in oxyfuel technology helps to prevent the emission of NO_x as an undesirable product of air-combustion technology

Table 1 summarizes the data of the flue gas conditions which provide critical insights into the characteristics of the flue gas leaving the combustion system in the cases of both air-combustion and oxyfuel-combustion technologies. The nitrogen portion is replaced with CO_2 as an inert gas. As carbon dioxide has a molecular weight larger than that of nitrogen, the mass flow of oxyfuel-combustion flue gases is larger. This alteration indicates the intentional adjustment of the combustion environment to enhance carbon capture efficiency by enriching the flue gas with CO_2 in oxyfuel-combustion.

https://doi.org/10.1021/acs.iecr.4c02216
Ind. Eng. Chem. Res. 2024, 63, 16486−16496

Table 1. Flue Gas Data Before the Capture Process

Parameter		Data
Temperature (°C)		120
Pressure (bar)		1.1
	Air-combustion	Oxyfuel-combustion
Flow rate (kg/s)	650	921.39
	Composition (Mole %)	
H_2O	8.0	8.0
N_2	76.0	2.0
O_2	12.0	12.0
CO_2	4.0	78.0

However, the amount of CO_2 originating from the fossil fuel burning process is always the same.

The CO_2-related characteristics of the simulation are demonstrated in Table 2. As outlined in the provided data,

Table 2. Main Results of the Carbon Capture Process

Plant data	Result
CO_2 capture ratio	90%
CO_2 feed content	40.38 kg/sec
Captured CO_2 flow rate	36.35 kg/sec

the CO_2 capture ratio, standing at 90%. The CO_2 feed content of 40.38 kg/s indicates the mass of carbon dioxide present in the flue gas, while the captured CO_2 flow rate of 36.35 kg/s signifies the amount successfully captured through the considered processes.

Chemistry and Mass Transfer. For all simulations, different thermodynamic assumptions are applied in the liquid and vapor phases. The electrolyte non-random two-liquid activity coefficient model coupled with the Redlich−Kwong equation of state (ELECNRTL-RK) and Henry's law for electrolyte systems has been selected and applied for liquid phase. As the ions are not assumed to be present in the vapor phase, the SRK EoS model is selected for the description of the thermodynamic behavior of this phase.

The following equilibrium and kinetic reactions are deemed for the MEA and water-based CO_2 capture and are described in Table 3.

The chemical equilibrium constant K_{eq} is calculated according to eq 1. In this equation, T is the absolute temperature, and A, B, C, and D are the constants.[41]

Table 3. Equilibrium and Kinetic Reactions for the CO_2 Capture Process

Reaction Name	Stoichiometry	Reaction No.
Equilibrium		
Amine protonation	$MEA + H_3O^+ \leftrightarrow MEAH^+ + H_2O$	(1)
Bicarbonate dissociation	$HCO_3^- + H_2O \leftrightarrow CO_3^{2-} + H_3O^+$	(2)
CO_2 hydrolysis	$CO_2 + 2H_2O \leftrightarrow HCO_3^- + H_3O^+$	(3)
Carbamate hydrolysis	$MEA + HCO_3^- \leftrightarrow MEACOO^- + H_2O$	(4)
Water dissociation	$2H_2O \leftrightarrow OH^- + H_3O^+$	(5)
Kinetic		
Bicarbonate formation	$CO_2 + OH^- \rightarrow HCO_3^-$	(6)
Carbamate formation	$MEA + CO_2 + H_2O \rightarrow MEACOO^- + H_3O^+$	(7)

$$\ln K_{eq} = A + \frac{B}{T} + C\cdot\ln T + D\cdot T \tag{1}$$

The equilibrium reactions are applied to all of the modules in the process simulation except for the absorber and stripper columns. These two columns control each stage kinetically. The rate of kinetic reactions is described by the power-law expression represented in eq 2, where r is the rate of reaction, k is the pre-exponential factor, T is the absolute temperature, R is the gas constant, and E is the activation energy. These values are reported according to the previous work.[41]

$$r_i = k_i\left[-\frac{E_j}{R}\cdot\left(\frac{1}{T}-\frac{1}{T_0}\right)\right] \tag{2}$$

In the case of capture with pressurized water, only reactions 2, 3, and 5 are being considered since these reactions use only pure water for the physical absorption of CO_2. Moreover, kinetic reactions are associated with only the chemical absorption of CO_2 by aqueous MEA.

Description of the Simulated Processes. This section introduces three types of research configurations: MEA-−CO_2 capture, H_2O−CO_2 capture, and H_2O−CO_2 capture + gas dehydration. The primary input parameters of the components and requirements utilized in model development are presented.

MEA−CO_2 Capture Process. A typical amine-based CO_2 absorption system consists of an absorber, a stripper, and a rich/lean heat exchanger. As shown in Figure 2, the 120 °C flue gas after the pretreatment section should be cooled to 40 °C before reaching the absorber column. It enters at the bottom of the absorber column and contacts with the countercurrent lean MEA solution. The rich MEA is pumped into the regeneration process then after the absorption it is preheated in the HX-1 with the lean solvent leaving the bottom of the stripper. A trim heat exchanger is applied to fix the optimal input temperatures of the rich solvent to the stripper.

Table 4 shows the main input parameters of the columns and specifications that are used for the model development of the absorber and stripper. The rate-based model is applied to model the absorber−stripper system as the comparison of experimental data and model analysis approved that it is more suitable than the equilibrium phase model.[41]

Table 5 offers critical characteristics for the MEA−CO_2 capture system's heat transfer procedures. In the air-combustion, the cooling heat exchangers of C-01 and C-02 exhibit power duties of 82.38 and 19.56 MW, respectively. The condenser, responsible for heat removal in this context, has a power duty of 76.45 MW. The heating heat exchanger of H-01 and the reboiler in the air-combustion scenario demand 43.09 and 174.37 MW, respectively. The oxy-fuel-combustion cooling and heating devices show similar trends, with C-01, C-02, and the condenser exhibiting varying power duties and temperatures. However, the reboiler duty associated with this technology is almost 30% lower than that of the air-combustion.

Table 6 outlines the technical characteristics of pressure changes within the MEA−CO_2 capture process, focusing on the pump efficiency set at 90%. In the air-combustion scenario, pump p-01 has a modest power duty of 0.08 MW, generating an outlet pressure of 2 bar and an outlet temperature of 38 °C. Similarly, in the oxyfuel-combustion case, the same pump (p-01) exhibits a slightly lower power duty of 0.06 MW with an

https://doi.org/10.1021/acs.iecr.4c02216
Ind. Eng. Chem. Res. 2024, 63, 16486−16496

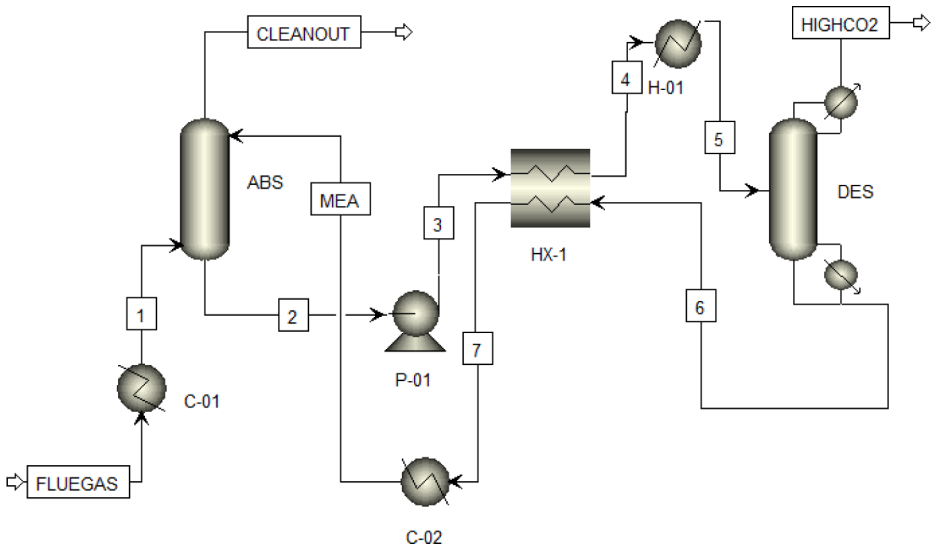

Figure 2. Configuration of the MEA-CO_2 capture process for air-combustion and oxy fuel-combustion.

Table 4. Model Specifications of Absorber and Stripper Column for the MEA-CO_2 Capture Plan

Parameter	Data
Absorbent features	
Absorbent	MEA
Lean solvent w/w	30%
Lean solvent temperature	40 °C
Lean solvent pressure	1.1 bar
Absorber and stripper	
Number of stages	15
Calculation type	Rate-based (RadFrac)
Condenser	Partial vaper
Reboiler	Kettle
Packing type	Mellapak, Sulzer, Standard, 250Y
Absorber packing height	20 m
Absorber packing diameter	15 m
Stripper packing height	22 m
Stripper packing diameter	12 m

Table 5. Specifications of Heat Transfer in the MEA−CO_2 Capture Process

Components	Power duty (MW)	Inlet T (°C)	Outlet (°C)
Air-combustion			
Cooling			
C-01	82.38	120	40
C-02	19.56	49	40
Condenser	76.45	101	101
Heating			
H-01	43.09	103	110
Reboiler	174.37	122	122
Oxyfuel-combustion			
Cooling			
C-01	96.76	120	40
C-02	14.90	49	40
Condenser	59.88	95	95
Heating			
H-01	51.35	99	110
Reboiler	120.66	122	122

Table 6. Technical Characteristics of Pressure Changes in MEA-CO_2 During the Process

(Pump efficiency = 90%)			
Components	Power duty (MW)	Outlet pressure (bar)	Outlet temperature (°C)
Air-combustion			
Consumption			
p-01	0.08	2	38
Oxyfuel-combustion			
Consumption			
p-01	0.06	2	39

outlet pressure of 2 bar and a slightly elevated outlet temperature of 39 °C.

H_2O−CO_2 Capture Process. The carbon capture procedure using H_2O was also investigated. The gas's solubility in water is proportional to Henry's constant and the gas's partial pressure. The higher the gas's partial pressure, the more CO_2 is absorbed by water. It has been reported that CO_2 has a substantially greater solubility in water than N_2 and O_2, implying that at the same partial pressure, water would absorb more CO_2. This phenomenon is used to separate CO_2 from the flue gas's other components.

The process design for the H_2O−CO_2 capture process is shown in Figure 3. The flue gas pressure at 120 °C was increased to 26 bar through two-stage compression. The outlet stream is initially cooled in the heat exchanger and cooled to 30 °C after the second compressor, then introduced into a counter-current 15-stage absorber (equilibrium-based model). Water (H_2O) is introduced into the absorber at 25.6 bar and 5 °C from above. The high-pressure clean gas (CL-GAS) exits from the top of the absorber. The temperature of this stream is increased to 370 °C by passing through a heat exchanger (HX-1) and producing power in an expander (EXP-01) by decreasing the gas pressure to atmospheric pressure. The rich CO_2 water exits the absorber from the bottom at 26 bar and 30 °C. Then, its pressure drops to 2 bar in the turbine (*T*-01) to generate electricity in the operation. In the desorber (DES) at 2 bar and 30 °C, a portion of absorbed CO_2 enters the gas phase and is recycled to the first stage of compression. The pressure of the CO_2-containing water is reduced to 1.1 bar

https://doi.org/10.1021/acs.iecr.4c02216
Ind. Eng. Chem. Res. 2024, 63, 16486−16496

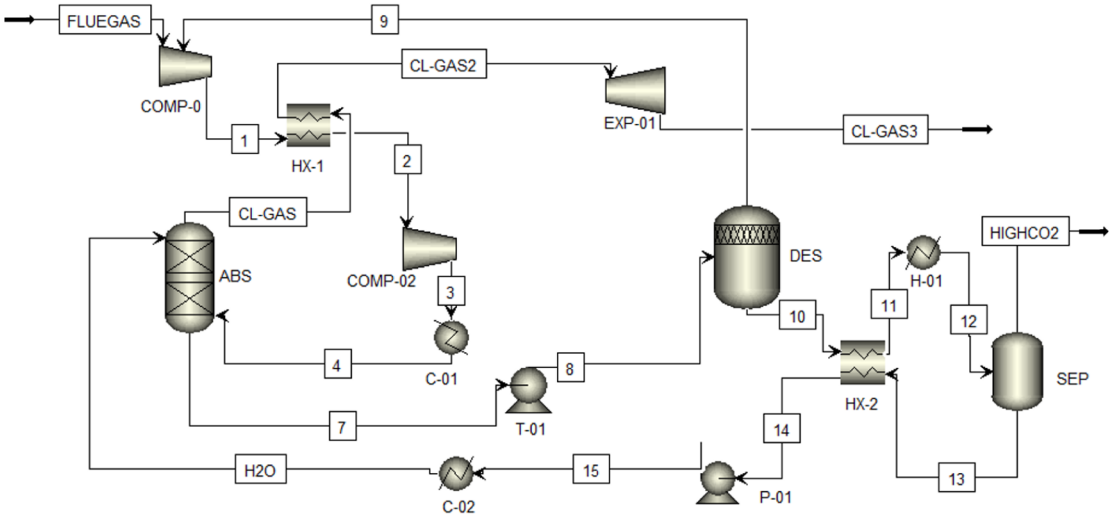

Figure 3. Process configuration of carbon capture with pressurized H_2O.

by a two-phase separation (SEP) to separate CO_2 from water and return water to the cycle by increasing pressure to 25.9 bar via a pump (*p*-01) and reducing temperature to 5 °C via a cooler (C-02).

Technical characteristics associated with pressure changes in the H_2O-CO_2 capture process are reported and compared in Table 7. In the air-combustion, COMP-01 and COMP-02, the compressors, exhibit substantial power duties of 230.60 and 131.22 MW, respectively, with varying outlet pressures of 8 and 26 bar. The pump (*p*-01) had a power consumption of 1.46 MW, generating an outlet pressure of 25.9 bar. On the generation side, EXP-01 and *T*-01, the expander and turbine, produce 205.40 and 1.60 MW, respectively, with controlled outlet pressure and temperature levels. Transitioning to the oxy-fuel-combustion scenario, similar trends are observed. COMP-01 and COMP-02 still exhibit high power duties, although slightly reduced, with notable variations in outlet temperatures. The pump (*p*-01) demonstrates a reduced power consumption of 0.43 MW, maintaining a similar outlet pressure.

Table 7. Technical Characteristics of Pressure Changes in the H_2O-CO_2 Capture Process

Components	(Compressors, expanders, and pump efficiency = 90%) Power duty (MW)	Outlet pressure (bar)	Outlet temperature (°C)
Air-combustion			
Consumption			
COMP-01	230.60	8	413
COMP-02	131.22	26	315
p-01	1.46	25.9	31
Generation			
EXP-01	205.40	1.1	45
T-01	1.60	1.1	30
Oxyfuel-combustion			
Consumption			
COMP-01	227.50	8	314
COMP-02	130.20	26	255
p-01	0.43	25.9	31
Generation			
EXP-01	209.60	1.1	45
T-01	1.22	1.1	30

The specifications of heat transfer associated with H_2O-CO_2 capture are provided in Table 8. Generally, cooler 1 (C-01) for the cooling of the high-pressure flue gas stream toward the absorber has the highest cold utility consumption in both technologies. On the heating side, H-01 exhibits a power duty of 18.47 MW, elevating the temperature from 45 to 50 °C, completing the thermal cycle for the air-combustion scenario. Shifting to the oxyfuel-combustion scenario, H-01, responsible for heating, operates with a power duty of 38.50 MW, elevating the temperature from 34 to 50 °C.

Table 8. Specifications of Heat Transfer in the H_2O-CO_2 Capture Process

Components	Power duty (MW)	Inlet T (°C)	Outlet (°C)
Air-combustion			
Cooling			
C-01	311.97	315	30
C-02	66.93	31	5
Heating			
H-01	18.47	45	50
Oxyfuel-combustion			
Cooling			
C-01	412.52	255	30
C-02	20.72	31	5
Heating			
H-01	38.50	34	50

H_2O-CO_2 Capture + Gas Dehydration Process. This work developed the H_2O-CO_2 capture process by adding gas dehydration before the gas compression section to reduce the electrical power demand of the process. The power plant's flue gas mostly consists of H_2O, CO_2, N_2, and O_2. When high-humidity flue gas is fed directly into the compression section, it may result in an increased power consumption. As a result, the solution should be pretreated before entering this section. The schematic diagram of flue gas dehydration is depicted in Figure 4. Initially, the flue gas from the power plant (120 °C, 1.1 bar) is cooled to near ambient temperature (30 °C). Then, the two-phase separation (Flash) is introduced, and the saturated water in the flue gas is translated into the liquid phase and ejected

https://doi.org/10.1021/acs.iecr.4c02216
Ind. Eng. Chem. Res. 2024, 63, 16486−16496

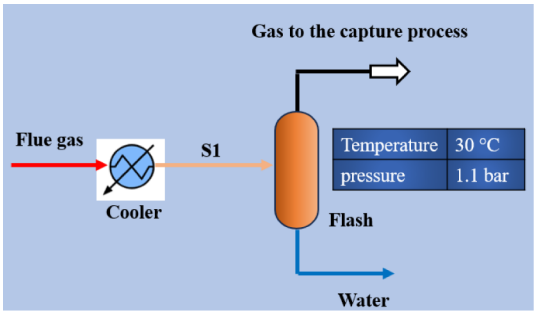

Figure 4. Schematic diagram of the flue gas dehydration process.

from the separator. The CO_2-riched stream is transferred to the capture process, and the separated water is eventually mixed with the recycled water and introduced to the absorber.

There is a conversion factor for the flue gas dehydration process that transforms the mole fraction and mass fraction of each component. The water flow rate of flue gas removal via the condenser is calculated as follows:

$$\dot{m}_{dw} = \dot{m}_{fg} x_{H_2O} \quad (3)$$

where $\dot{m}_{fg}$ is the mass flow rate of the flue gas and x_{H_2O} is the mass fraction of water in the flue gas. After flue gas dehydration, the mole ratio of the remaining CO_2-rich stream will change.

Figure 5 depicts the H_2O-CO_2 capture process, which consists of gas dehydration. The red dotted box indicates the position of the dehydration phase before the compression.

Table 9 shows the pressure changes in the H_2O-CO_2 capture process when it is combined with gas dehydration. The power duty of compressors in both technologies, air-combustion and oxyfuel-combustion, is much lower than that of the initial H_2O-CO_2 capture process. This decrease occurs because of the use of gas dehydration before the primary capture procedure. In the air-combustion scenario, COMP-01 and COMP-02 have power duties of 169.04 MW and 100.53 MW, respectively. These compressors operate at outlet pressures of 8 and 26 bar, the same as previous models.

Table 9. Technical Characteristics of Pressure Changes in H_2O-CO_2 Capture + Gas Dehydration

(Compressors, expanders, and pump efficiency = 90%)			
Component	Power duty (MW)	Outlet pressure (bar)	Outlet temperature (°C)
Air-combustion			
Consumption			
COMP-01	169.04	8	266
COMP-02	100.53	26	124
p-01	1.46	25.9	31
Generation			
EXP-01	202.32	1.1	45
T-01	1.58	1.1	30
Oxyfuel-combustion			
Consumption			
COMP-01	158.89	8	200
COMP-02	91.05	26	82
p-01	0.33	25.9	31
Generation			
EXP-01	213.52	1.1	45
T-01	0.78	1.1	30

The power duties for COMP-01 and COMP-02 in the oxyfuel-combustion scenario are somewhat lower than in the air-combustion scenario.

Table 10 details the specifications of the heat transfer process within H_2O-CO_2 capture coupled with a gas dehydration system. Compared to previous models, here is one additional cooler (C-03), associated with the gas dehydration process. In the air-combustion cooling system, C-01, C-02, and C-03 exhibit power duties of 93.22, 67.24, and 113.60 MW, respectively. These cooling components play a vital role in managing the elevated temperatures associated with air combustion. On the heating side, H-01 has a power duty of 17.65 MW, elevating the temperature from 46 to 50 °C, completing the thermal cycle for the air-combustion scenario. In the oxyfuel-combustion scenario, similar trends are observed. C-01, C-02, and C-03 still exhibit impressive cooling capabilities.

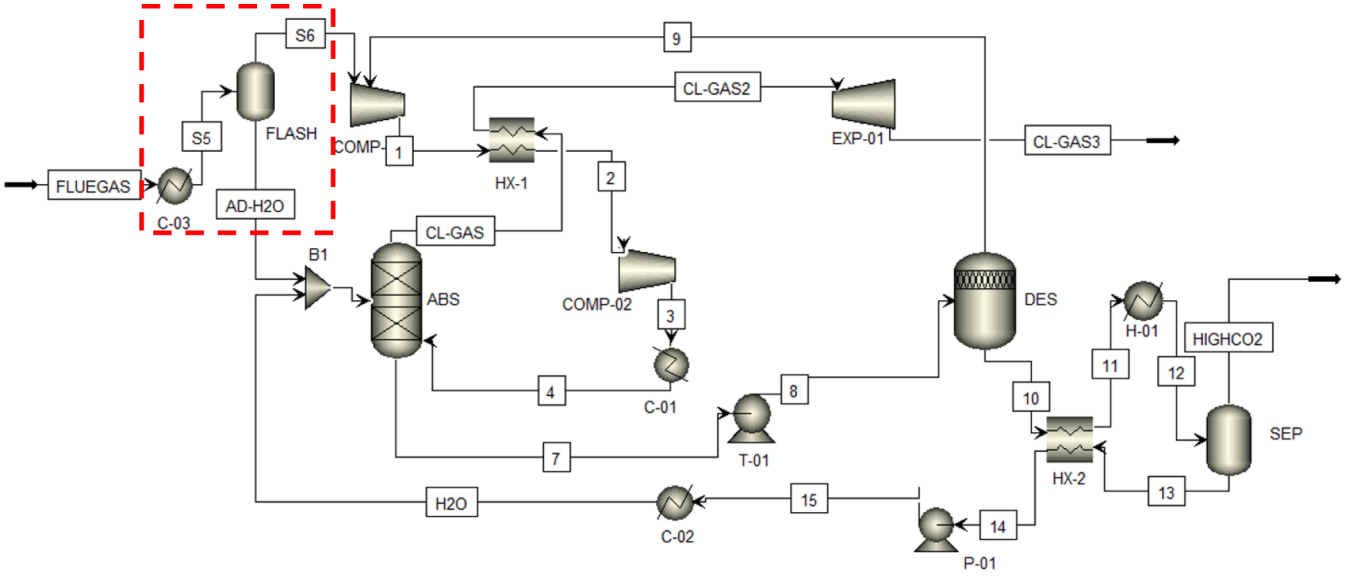

Figure 5. Process configuration of carbon capture with H_2O + gas dehydration, red dotted area is associated with gas dehydration process.

https://doi.org/10.1021/acs.iecr.4c02216
Ind. Eng. Chem. Res. 2024, 63, 16486−16496

Table 10. Specifications of Heat Transfer in H_2O-CO_2 Capture + Gas Dehydration

Component	Power duty (MW)	Inlet T (°C)	Outlet (°C)
	Air-combustion		
Cooling			
C-01	93.22	124	30
C-02	67.24	31	5
C-03	113.60	120	30
Heating			
H-01	17.65	46	50
	Oxyfuel-combustion		
Cooling			
C-01	89.15	81	30
C-02	15.64	31	5
C-03	158.19	120	30
Heating			
H-01	28.85	35	50

Utility Consumption. Utilities such as electricity, water, steam, and gas are essential for running equipment and machinery and maintaining the right environmental conditions. Inefficient utility consumption can result in increased expenditures and worse profitability. To investigate the total heating, cooling, and electricity utility requirements at process conditions, the utility dashboard in Aspen Plus was activated, the results are indicated in Table 11. Electricity utility costs encompass both heating and cooling (cooling water and refrigerant 1) expenses. Each utility part is used to provide power associated with the components of the considered methods in this study, as reported in Tables 5−10.

Table 11. Default Utility Selection of Aspen Plus for Processes

Utility	Inlet T (°C)	Outlet T (°C)	Cost ($/MWh)	Deployment
Cooling water	20	30	0.76	Cooling components with an outlet temperature higher than 30 °C
Refrigerant 1	−25	−24	7.92	Cooling components with an outlet temperature lower than 20 °C
Steam (MP)	180	170	9.86	Heating components
Electricity			77.50	(Consumption − Generation) + electricity of refrigeration cycle

RESULT AND DISCUSSION

Detailed Utility Demand Comparison. Table 12 presents a comprehensive breakdown of detailed utility consumption for various carbon capture methods, considering heating, cooling (cooling water and refrigerant), and electricity requirements. Electricity demands are calculated as the total consumption subtracted from the generation during the CO_2 capture process, which must be supplied by the utility sector. As a general trend for air- and oxyfuel-combustion, the MEA−CO_2 capture process exhibits substantial heating and cooling requirements, but it does not demand additional electricity. In contrast, the H_2O-CO_2 capture process involves significantly higher cooling demands, mainly due to the substantial power duty associated with the cooling components. The addition of gas dehydration in the H_2O-CO_2 capture process reduces the cooling and electricity demands. This reduction is particularly noticeable in cooling water usage, highlighting the potential benefits of incorporating dehydration in terms of resource efficiency.

Table 12. Detailed Utility Consumption of the Considered Capture Methods

Method	Heating (MW)	Cooling (MW)		Electricity (MW)
	Steam	Cooling water	Refrigerant 1	
	Air-combustion			
MEA−CO_2 capture	217.46	178.39	0	0.08
H_2O-CO_2 capture	18.47	311.97	66.93	156.28
H_2O-CO_2 capture + gas dehydration	17.65	206.82	67.24	61.13
	Oxyfuel-combustion			
MEA−CO_2 capture	172.01	171.54	0	0.06
H_2O-CO_2 capture	38.50	412.52	20.72	147.31
H_2O-CO_2 capture + gas dehydration	28.85	247.34	15.64	35.97

Aggregated Utility Requirement and Its Corresponding Cost. Figure 6 demonstrates a comprehensive overview of the total utility demand and associated costs. In the air-combustion scenario, the MEA−CO_2 capture process has an approximately total utility demand of 395 MWh and incurs a total utility cost of 20 M$/year. The H_2O-CO_2 capture process exhibits a higher total utility demand, leading to a higher total utility cost of 114 M$/year. However, the integration of gas dehydration in the H_2O-CO_2 capture process results in a notable reduction in both total utility demand (352 MWh) and cost (49 M$/year), suggesting improved economic and resource efficiency. Regarding the oxyfuel-combustion scenario, the MEA−CO_2 capture process has a total utility demand of 343 MWh and a total utility cost of 16 M$/year. The H_2O-CO_2 capture process shows a higher total utility demand (620 MWh) and cost (107 M$/year). Like the air-combustion case, the integration of gas dehydration in the H_2O-CO_2 capture process results in substantial reductions in both total utility demand and cost. The results emphasize the significant impact of incorporating gas dehydration on the overall utility demand (almost 35% and 45% reduction for air and oxyfuel-combustion, respectively) and associated costs (around 55% for air-combustion and 70% for oxyfuel-combustion) for both combustion scenarios in pressurized-water CO_2 capture methods. But still, the cost of H_2O-CO_2 capture coupled with the gas dehydration method is significantly higher than that of MEA−CO_2 capture.

Electricity Demands in H_2O-CO_2 Capture Process. Contribution to electricity power generation and consumption within the H_2O-CO_2 capture method for both air-combustion and oxyfuel-combustion technologies is shown in Figure 7. In air-combustion, electricity consumption is measured at 363.28 MW, while generation is 207 MW. The resulting utility demand, representing the net electricity needs of the process, is calculated at 156.28 MW. Similarly, in the oxyfuel-combustion scenario, the electricity consumption decreases slightly to 358.13 MW, and generation increases to 210.82 MW. Despite the increase in generation, utility demand decreased to 147.31 MW. This indicates an impact of combustion technology on the electricity demand of the H_2O-CO_2 capture process.

Electricity Demands in H_2O-CO_2 + Gas Dehydration Capture Method. The share of electricity power generation and consumption in the H_2O-CO_2 capture coupled with the

https://doi.org/10.1021/acs.iecr.4c02216
Ind. Eng. Chem. Res. 2024, 63, 16486−16496

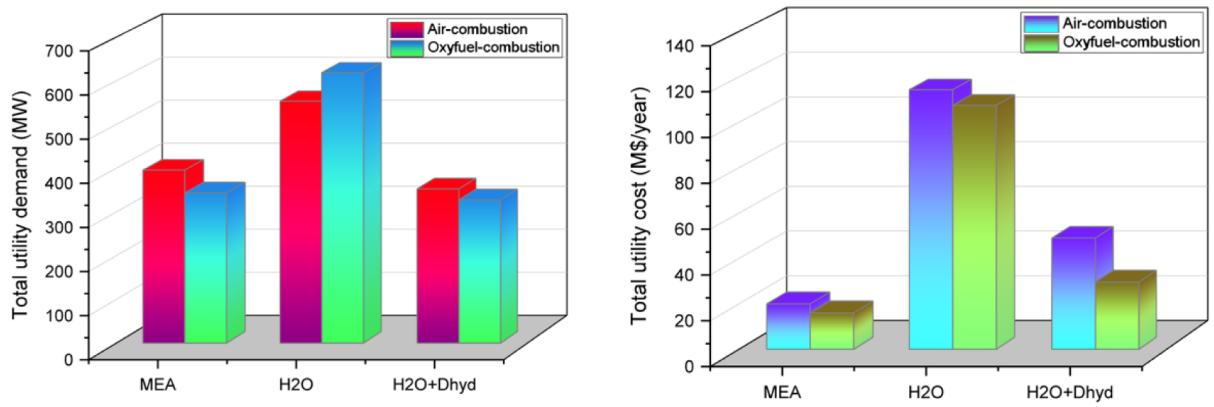

Figure 6. Total utility demand (left) and associated costs (right) of the considered capture methods.

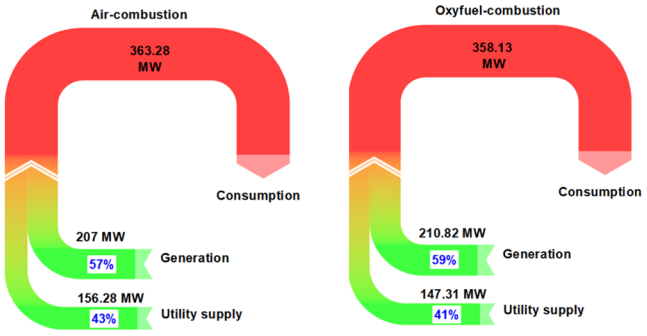

Figure 7. Contribution to electricity power generation and consumption in the H_2O-CO_2 capture method.

gas dehydration method depict in Figure 8. In the air-combustion, electricity consumption is measured at 271.03

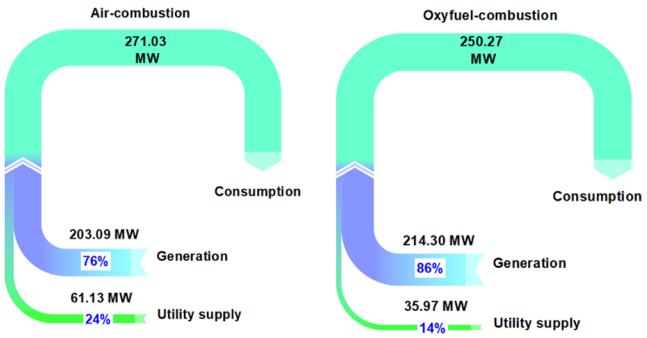

Figure 8. Contribution of electricity power generation and consumption in the H_2O-CO_2 capture + gas dehydration method.

MW, generation at 203.9 MW, resulting in a utility demand of 61.13 MW. Compared to the former case, here, there is an approximately 60% and 75% reduction in the utility demands. This suggests that the integration of gas dehydration has a significant impact on reducing the overall electricity demand compared to the H_2O-CO_2 capture method without gas dehydration.

Regarding the oxyfuel-combustion technology, the utility demand further decreases to 35.97 MW. This suggests that the benefits of gas dehydration in terms of energy efficiency extend to different combustion technologies.

The Impact of Gas Dehydration on Electrical Utility Demand and Water Circulation. Figure 9 shows the impact of the gas dehydration process temperature on the electricity demand and water circulation. The results present a clear correlation between the dehydration process temperature, electricity utility demand, and water content of the feed at the dehydration. As the dehydration temperature increases from 30 to 120 °C, there is a consistent rise in electricity demand. This indicates that higher temperatures in the dehydration process demand more energy for its operation.

In contrast, the water content of the feed gas shows a distinct pattern. Initially, at lower temperatures (30−45 °C), the amount of liquid water is significant, steadily decreasing until it goes down to zero at 50 °C and remains there at higher temperatures. The findings underscore the importance of optimizing the dehydration process temperature to achieve a balance between the electricity utility demand and water.

Solvent Consumption of Each Capture Method. The absorbent consumption in the three simulations studied is reported in Figure 10. As a general trend, the absorbent flow rates of oxyfuel combustion are lower than those of air combustion. The primary reason is that the carbon dioxide concentration in oxyfuel combustion is significantly higher than that of air combustion, resulting in a greater driving force for mass transfer and a lower solvent need.

Regarding the H_2O-CO_2 capture process, the H_2O flow rate in air combustion is roughly four times greater than that of oxyfuel technology. When gas dehydration is added to the pressurized water capture process, the water demand in the absorber tower increases, which may be met by supplying the separated water from the dehydration process to this component.

According to Figure 11, which shows the water flow of the CO_2 capture and the gas dehydration method for air and oxyfuel-combustion technologies at the flash condition (30 °C and 1.1 bar), the H_2O separated from the flue gas in air combustion and oxyfuel-combustion is 21 and 22 kg/s, respectively. When these values are split by the total water demand, water from dehydration may supply between 4% and 17% of the total water demand of air combustion and oxyfuel-combustion processes, respectively. Therefore, the oxy-fuel-combustion process consumes 105 kg/s of pure water, which is 15 kg/s less than the initial H_2O-CO_2 capture method.

Comparison of Total CO_2 Emissions in Considered Carbon Capture Methods. Figure 12 illustrates the overall CO_2 emissions associated with utility components for different carbon capture methods. These values are calculated using the Aspen utility data package, based on the detailed utility consumption outlined in Table 12 and the emission factors

https://doi.org/10.1021/acs.iecr.4c02216
Ind. Eng. Chem. Res. 2024, 63, 16486−16496

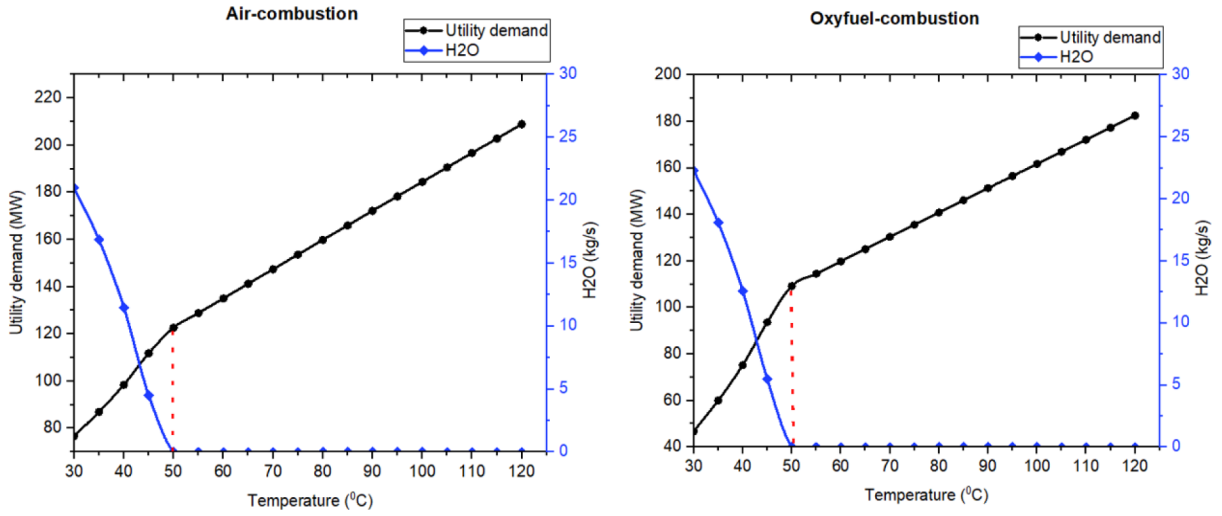

Figure 9. Impact of the gas dehydration temperature on the electrical utility demand and water circulation.

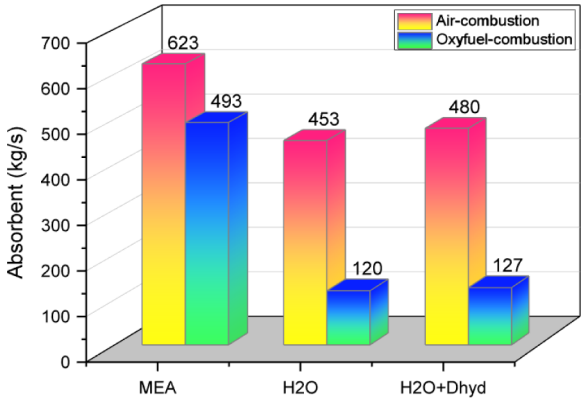

Figure 10. Solvent flow rates in the considered carbon capture methods.

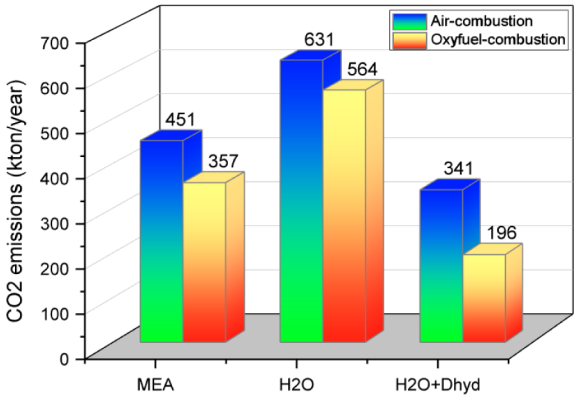

Figure 12. CO_2 emissions are associated with utility consumption for considered configurations.

assigned to each utility component within the Aspen simulation.

In air combustion, the MEA−CO_2 capture method generates 451 kton of CO_2 emissions annually, while H_2O−CO_2 capture and H_2O−CO_2 capture with gas dehydration result in 631 and 341 kton of CO_2 emissions per year, respectively.

For oxyfuel combustion, MEA−CO_2 capture yields 357 kton of CO_2 emissions, H_2O−CO_2 capture results in 564 kton annually, and H_2O−CO_2 capture with gas dehydration contributes 196 kton of CO_2 emissions each year. These findings highlight the potential environmental benefits of H_2O−CO_2 capture with gas dehydration methods, suggesting a more environmentally friendly approach to reducing CO_2 emissions across different combustion technologies.

CONCLUSIONS

A comparison of the efficiencies of absorbents, pressurized water, and MEA solution is carried out for carbon capture. Both absorbents are used in industrial practice; as long as the water is applied in the ammonia technology, the MEA solutions are favored for decarbonization of flue gases.

In the case of water application, the dehydration of the gas before carbon capture significantly reduces energy consumption, consequently leading to lower CO_2 emissions and costs associated with energy consumption. The calculation of

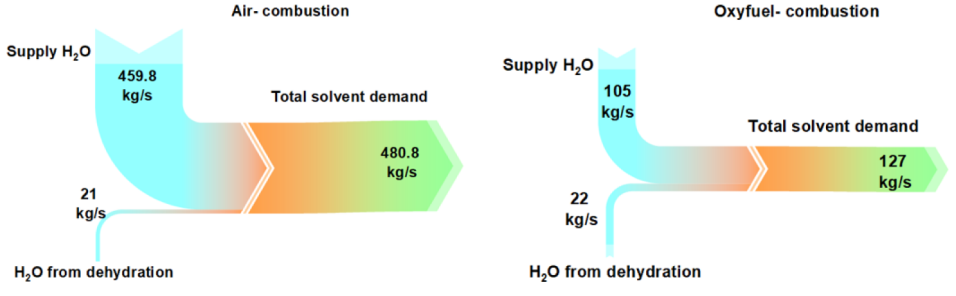

Figure 11. Water flows in the H_2O−CO_2 capture + gas dehydration method.

https://doi.org/10.1021/acs.iecr.4c02216
Ind. Eng. Chem. Res. 2024, 63, 16486−16496

electricity demand shows that the Figure of the H_2O-CO_2 capture method is higher than that of the $MEA-CO_2$ alternative, leading to a higher cost of energy.

Employing gas dehydration in the H_2O-CO_2 capture process results in 60% and 75% decreases in electrical power demand for air and oxyfuel-combustion, respectively. The CO_2 emissions associated with utility consumption in H_2O-CO_2 capture with gas dehydration methods are lower than those of other alternatives.

The main drawback can be related to the higher electricity demands in the water-based carbon capture process that can directly impact the cost of utility supply. However, it is highly dependent on the method of electricity production. Therefore, the application of water as absorbent for carbon capture might be considered if the electricity is cheap, e.g., originating from renewable sources. Another merit is that the water is more environmentally friendly and user-friendly than an amine solution. So, water as an absorbent can be seriously considered in the case of engineering design.

AUTHOR INFORMATION

Corresponding Author

Saeed Talei − *Institute of Chemistry and Higher Education and Industrial Cooperation Centre, University of Miskolc, Miskolc H-3515, Hungary*; orcid.org/0000-0003-4116-2332; Email: talei.saeed@uni-miskolc.hu

Authors

Agnes Szanyi − *Institute of Chemistry, University of Miskolc, Miskolc H-3515, Hungary; Department of Chemical and Environmental Process Engineering, Budapest University of Technology and Economics, Budapest H-1521, Hungary*

Peter Mizsey − *Higher Education and Industrial Cooperation Centre, University of Miskolc, Miskolc H-3515, Hungary*

Complete contact information is available at: https://pubs.acs.org/10.1021/acs.iecr.4c02216

Notes

The authors declare no competing financial interest.

ACKNOWLEDGMENTS

The authors appreciate the financial support of the Stipendium Hungaricum program, the Hungarian Scientific Research Funds OTKA 128543, and the LIFE19 CCA/HU/001320 − LIFE-CLIMCOOP project supported by EU LIFE program.

REFERENCES

(1) Xu, R.; Kim, S.; Ahn, H.; Kim, H. S.; Lee, J. W.; Kang, Y. T. A General Energy-Efficient Strategy for Optimizing CO2 Capture: Designing and Harnessing the Rapid Adsorption Kinetics of Amine-Impregnated Adsorbents. *Sep. Purif. Technol.* **2024**, *347*, 127668.

(2) Talei, S.; Soleimani, Z. An Overview of Bioenergy with Carbon Capture and Storage Process as a Negative Emission Technology. *J. Environ., Agric. Biol. Sci.* **2021**, *3* (1), 1−11.

(3) Talei, S.; Soleimani, Z. Comparative Analysis of Three Different Negative Emission Technologies, BECCS, Absorption and Adsorption of Atmospheric CO. *Civ. Environ. Eng. Rep.* **2021**, *31* (3), 99−117.

(4) Gao, C.; Feng, J.; Mo, W.; Guo, W.; Ma, S.; Su, X.; Yang, J.; Wang, D.; Sun, W.; Jia, H.; He, A. Experimental Testing and Mechanism Investigation of Amine-Functionalized Layered Vermiculite for CO2 Capture. *Sep. Purif. Technol.* **2024**, *348*, 127756.

(5) Yan, Z.; Zheng, W.; Liu, S.; Luo, X.; Huang, Y.; Jin, B.; Gao, H.; Xiao, M.; Liang, Z. Process Simulation and Optimization for Post-Combustion CO2 Capture Pilot Plant Using High CO2 Concentration Flue Gas as a Source. *Sep. Purif. Technol.* **2024**, *349*, 127873.

(6) Hills, T.; Leeson, D.; Florin, N.; Fennell, P. Carbon Capture in the Cement Industry: Technologies, Progress, and Retrofitting. *Environ. Sci. Technol.* **2016**, *50* (1), 368−377.

(7) Silveira, B. H. M.; Costa, H. K. M.; Santos, E. M. Bioenergy with Carbon Capture and Storage (BECCS) in Brazil: A Review. *Energies* **2023**, *16* (4), 2021.

(8) Lu, S.; Zhang, J.; Lang, L.; Hou, T.; Yang, F.; Shen, C.; Liu, H.; Liu, L.; Kang, G. Amino Acids to Reduce the Escape of Organic Amines in the CO2 Capture Process. *Sep. Purif. Technol.* **2024**, *350*, 127659.

(9) Dees, J.; Oke, K.; Goldstein, H.; McCoy, S. T.; Sanchez, D. L.; Simon, A. J.; Li, W. Cost and Life Cycle Emissions of Ethanol Produced with an Oxyfuel Boiler and Carbon Capture and Storage. *Environ. Sci. Technol.* **2023**, *57* (13), 5391−5403.

(10) Schmidt, J.; Leduc, S.; Dotzauer, E.; Schmid, E. Cost-Effective Policy Instruments for Greenhouse Gas Emission Reduction and Fossil Fuel Substitution through Bioenergy Production in Austria. *Energy Policy* **2011**, *39* (6), 3261−3280.

(11) Bhown, A. S.; Freeman, B. C. Analysis and Status of Post-Combustion Carbon Dioxide Capture Technologies. *Environ. Sci. Technol.* **2011**, *45* (20), 8624−8632.

(12) Nagy, T.; Mizsey, P. Model Verification and Analysis of the CO2-MEA Absorber−Desorber System. *Int. J. Greenhouse Gas Control.* **2015**, *39*, 236−244.

(13) Ostovari, H.; Müller, L.; Skocek, J.; Bardow, A. From Unavoidable CO2 Source to CO2 Sink? A Cement Industry Based on CO2 mineralization. *Environ. Sci. Technol.* **2021**, *55* (8), 5212−5223.

(14) Talei, S.; Szanyi, A.; Mizsey, P. Improving the energy efficiency of carbon capture process: the thermodynamic insight. *Energy* **2024**, *308*, 133013.

(15) Nittaya, T.; Douglas, P. L.; Croiset, E.; Ricardez-Sandoval, L. A. Dynamic Modelling and Control of MEA Absorption Processes for CO2 Capture from Power Plants. *Fuel* **2014**, *116*, 672−691.

(16) Liu, Z.; Wang, L.; Kong, X.; Li, P.; Yu, J.; Rodrigues, A. E. Onsite CO2 Capture from Flue Gas by an Adsorption Process in a Coal-Fired Power Plant. *Ind. Eng. Chem. Res.* **2012**, *51* (21), 7355−7363.

(17) Song, C.; Liu, Q.; Deng, S.; Li, H.; Kitamura, Y. Cryogenic-Based CO2 Capture Technologies: State-of-the-Art Developments and Current Challenges. *Renewable Sustainable Energy Rev.* **2019**, *101*, 265−278.

(18) Kruber, B.; Droste, K.; Skiborowski, M. Thermodynamic Efficiency of Membrane-assisted Distillation Processes. *AichE J.* **2023**, *69* (6), No. e18015.

(19) Nagy, T.; Mizsey, P. Effect of Fossil Fuels on the Parameters of CO2 Capture. *Environ. Sci. Technol.* **2013**, *47* (15), 8948−8954.

(20) Garcia, M.; Knuutila, H. K.; Gu, S. ASPEN PLUS Simulation Model for CO2 Removal with MEA: Validation of Desorption Model with Experimental Data. *J. Environ. Chem. Eng.* **2017**, *5* (5), 4693−4701.

(21) House, K. Z.; House, C. H.; Schrag, D. P.; Aziz, M. J. Electrochemical Acceleration of Chemical Weathering as an Energetically Feasible Approach to Mitigating Anthropogenic Climate Change. *Environ. Sci. Technol.* **2007**, *41* (24), 8464−8470.

(22) Nessi, E.; Papadopoulos, A. I.; Seferlis, P. A Review of Research Facilities, Pilot and Commercial Plants for Solvent-Based Post-Combustion CO2 Capture: Packed Bed, Phase-Change and Rotating Processes. *Int. J. Greenhouse Gas Control* **2021**, *111*, 103474.

(23) Morgan, J. C.; Chinen, A. S.; Anderson-Cook, C.; Tong, C.; Carroll, J.; Saha, C.; Omell, B.; Bhattacharyya, D.; Matuszewski, M.; Bhat, K. S.; et al. Development of a Framework for Sequential Bayesian Design of Experiments: Application to a Pilot-Scale Solvent-Based CO2 Capture Process. *Appl. Energy* **2020**, *262*, 114533.

(24) Idem, R.; Wilson, M.; Tontiwachwuthikul, P.; Chakma, A.; Veawab, A.; Aroonwilas, A.; Gelowitz, D. Pilot Plant Studies of the CO2 Capture Performance of Aqueous MEA and Mixed MEA/

MDEA Solvents at the University of Regina CO2 Capture Technology Development Plant and the Boundary Dam CO2 Capture Demonstration Plant. *Ind. Eng. Chem. Res.* **2006**, *45* (8), 2414−2420.
(25) Frimpong, R. A.; Johnson, D.; Richburg, L.; Hogston, B.; Remias, J. E.; Neathery, J. K.; Liu, K. Comparison of Solvent Performance for CO2 Capture from Coal-Derived Flue Gas: A Pilot Scale Study. *Chem. Eng. Res. Des.* **2013**, *91* (6), 963−969.
(26) Kim, S.; Ko, Y.; Lee, G. J.; Lee, J. W.; Xu, R.; Ahn, H.; Kang, Y. T. Sustainable Energy Harvesting from Post-Combustion CO2 Capture Using Amine-Functionalized Solvents. *Energy* **2023**, *267*, 126532.
(27) Panda, D.; Kulkarni, V.; Singh, S. K. Evaluation of Amine-Based Solid Adsorbents for Direct Air Capture: A Critical Review. *React. Chem. Eng.* **2022**, *8* (1), 10−40.
(28) Basnayake, S. A.; Su, J.; Zou, X.; Balkus, K. J., Jr. Carbonate-Based Zeolitic Imidazolate Framework for Highly Selective CO2 Capture. *Inorg. Chem.* **2015**, *54* (4), 1816−1821.
(29) Pachitsas, S.; Bonalumi, D. Parametric Investigation of CO2 Capture from Industrial Flue Gases Using Aqueous Mixtures of Ammonia (NH3) and Potassium Carbonate (K2CO3). *Int. J. Greenhouse Gas Control* **2022**, *114*, 103567.
(30) Deng, D.; Deng, X.; Duan, X.; Gong, L. Protic Guanidine Isothiocyanate plus Acetamide Deep Eutectic Solvents with Low Viscosity for Efficient NH3 Capture and NH3/CO2 Separation. *J. Mol. Liq.* **2021**, *324*, 114719.
(31) Ramezani, R.; Mazinani, S.; Di Felice, R. State-of-the-Art of CO2 Capture with Amino Acid Salt Solutions. *Rev. Chem. Eng.* **2022**, *38* (3), 273−299.
(32) Haghbakhsh, R.; Raeissi, S. Deep Eutectic Solvents for CO2 Capture from Natural Gas by Energy and Exergy Analyses. *J. Environ. Chem. Eng.* **2019**, *7* (6), 103411.
(33) Lian, S.; Song, C.; Liu, Q.; Duan, E.; Ren, H.; Kitamura, Y. Recent Advances in Ionic Liquids-Based Hybrid Processes for CO2 Capture and Utilization. *J. Environ. Sci.* **2021**, *99*, 281−295.
(34) Zhang, Q.; Turton, R.; Bhattacharyya, D. Development of Model and Model-Predictive Control of an MEA-Based Postcombustion CO2 Capture Process. *Ind. Eng. Chem. Res.* **2016**, *55* (5), 1292−1308.
(35) Zhang, Y.; Que, H.; Chen, C.-C. Thermodynamic Modeling for CO2 Absorption in Aqueous MEA Solution with Electrolyte NRTL Model. *Fluid Phase Equilib.* **2011**, *311*, 67−75.
(36) Kervévan, C.; Beddelem, M.-H.; O'neil, K. CO2-DISSOLVED: A Novel Concept Coupling Geological Storage of Dissolved CO2 and Geothermal Heat Recovery−Part 1: Assessment of the Integration of an Innovative Low-Cost, Water-Based CO2 Capture Technology. *Energy Proc.* **2014**, *63*, 4508−4518.
(37) Bayramŏlu, K. Evaluation of Decarbonization Methods on Ships. *J. Mar. Eng. Technol.* **2023**, *3* (1), 20−33.
(38) Chen, L.; Zhang, L.; Wang, Y.; Xie, M.; Yang, H.; Ye, K.; Mohtaram, S. Design and Performance Evaluation of a Novel System Integrating Water-Based Carbon Capture with Adiabatic Compressed Air Energy Storage. *Energy Convers. Manage.* **2023**, *276*, 116583.
(39) Plus, A. *Rate Based Model of the CO2 Capture Process by MEA Using Aspen Plus*; Aspen Technology Inc.: Cambridge, MA, USA, 2008.
(40) Pérez-Calvo, J.-F.; Sutter, D.; Gazzani, M.; Mazzotti, M. Advanced Configurations for Post-Combustion CO2 Capture Processes Using an Aqueous Ammonia Solution as Absorbent. *Sep. Purif. Technol.* **2021**, *274*, 118959.
(41) Talei, S.; Fozer, D.; Varbanov, P. S.; Szanyi, A.; Mizsey, P. Oxyfuel Combustion Makes Carbon Capture More Efficient. *ACS Omega* **2024**, *9* (3), 3250−3261.

https://doi.org/10.1021/acs.iecr.4c02216
Ind. Eng. Chem. Res. 2024, 63, 16486−16496